A. Brömme, C. Busch, A. Dantcheva, C. Rathgeb and A. Uhl (Eds.): BIOSIG 2018,
Lecture Notes in Informatics (LNI), Gesellschaft für Informatik, Bonn 2018 1

Longitudinal Finger Rotation - Problems and Effects in Finger-Vein Recognition

Bernhard Prommegger[1], Christof Kauba[1] and Andreas Uhl[1]

Abstract: Finger-vein scanners or vein-based biometrics in general are becoming more and more popular. Commercial off-the-shelf finger-vein scanners usually capture only one finger from the palmar side using transillumination. Most scanners have a contact area and a finger-shaped support where the finger has to be placed onto in order to prevent misplacements of the finger including shifts, planar rotation and tilts. However, this is not able to prevent rotation of the finger along its longitudinal axis (also called non-planar finger rotation). This kind of finger rotation poses a severe problem in finger-vein recognition as the resulting vein image may represent entirely different patterns due to the perspective projection. We evaluated the robustness of several finger-vein recognition schemes against longitudinal finger rotation. Therefore, we established a finger-vein data set exhibiting longitudinal finger rotation in steps of 1° covering a range of ±90°. Our experimental results confirm that the performance of most of the simple recognition schemes rapidly decreases for more than 10° of rotation, while more advanced schemes are able to handle up to 30°.

Keywords: Longitudinal Finger Rotation, Finger-Vein Recognition, Multi-Perspective Finger-Vein Data Set, Performance Evaluation, Finger Vein Scanner Device

1 Introduction

Vascular pattern based biometrics, commonly denoted as vein biometrics, provide several advantages over other, well-established biometric recognition systems. Especially hand- and finger-vein based systems tend to replace fingerprint based ones in some application areas. Vein based systems rely on the structure of the vascular pattern formed by the blood vessels inside the human body tissue, which becomes visible in near-infrared (NIR) light only. This vessel structure is within the human body and thus vein based systems are insensitive to abrasion and skin surface conditions. Moreover, a liveness detection can be performed easily [KZ12].

However, finger-vein recognition systems are far from being perfect in terms of accuracy, reliability and usability. Their recognition performance may suffer from different internal and external factors which might lead to a lower performance. Internal factors include the configuration of the scanner itself, the illumination source and the NIR camera. Most of the internal and external factors impacting the finger-vein recognition performance can be ruled out by means of adding components to the scanner or tuning the scanner settings. External factors can be divided into environmental ones, including ambient light, dust or dirt on the sensor, high humidity, electromagnetic radiation, etc. and factors regarding the

[1] Department of Computer Sciences, University of Salzburg, AUSTRIA,
{bprommeg, ckauba, uhl}@cs.sbg.ac.at

presentation of the finger to the scanner device. The latter includes finger movement during acquisition and finger misplacement in general. Some of the environmental factors can be ruled out by using additional components for the vein scanner, e.g. the influence ambient light can be reduced by installing an NIR pass-through filter. However, especially tilt and rotation of the finger along its longitudinal axis (which are a form or finger misplacement) are hard to tackle. While the tilt can be avoided to a certain extent, as soon as there is only one finger to be captured, it is hard to avoid rotation of the finger along its longitudinal axis, especially for touchless finger-vein scanners, but not restricted to touchless operation. Hence, this is one of the main factors influencing the recognition performance of finger-vein systems in practical applications and it would be desirable if finger vein recognition schemes are able to tolerate such a rotation at least to a certain extent. To the best of our knowledge no systematic investigation of this particular problem has been performed so far. The analysis of these and other factors impacting the recognition performance of finger-vein recognition systems can be summarised as robustness analysis.

Some authors state that there is the problem of finger rotation along the longitudinal axis, which is also called out-plane finger rotation or non-planar rotation, while others claim that their recognition scheme is able to tolerate this up to a certain degree. Matsuda et al. [Ma16] claim that their recognition scheme is robust against this kind of finger misplacement. They did experiments and showed that their scheme is robust against these rotations up to $\pm 30°$, but their test data set, which is not publicly available, only consisted of vein images captured from 5 different people. Chen et al. [Ch18] proposed an approach to correct different types of finger deformations based on a finger geometric analysis. Their work includes finger rotation along the longitudinal axis as well (they call it type 3 deformation). They showed that by a non-linear correction of the finger rotation the recognition performance can be improved. However, they only estimate the amount of deformation, i.e. the rotation angle, while there is no ground-truth information of the actual rotation angle available.

The main contribution of our work is a systematic robustness evaluation of several finger vein recognition schemes against the finger's longitudinal rotation. In order to investigate the impact of longitudinal finger rotation a suitable data set is needed. Unfortunately, there is no such data set available, mainly because a specifically designed finger-vein scanner device is mandatory to acquire one. Thus, we established a finger rotation data set, exhibiting transillumination finger-vein images captured in different rotation angles in $1°$ steps in a range of $\pm 90°$ starting from the palmar view. This data set was captured using our custom designed, multi-perspective finger-vein scanner device and will be made publicly available in the future. Our experimental results show that longitudinal finger rotation poses a severe problem for most finger-vein recognition schemes.

The rest of this paper is organised as follows: Section 2 illustrates the problem of the finger's longitudinal rotation in detail. Section 3 presents our multi-perspective finger-vein scanner device and the finger rotation data set. Section 4 describes the experimental set-up and presents the performance evaluation results together with a results discussion. Section 5 concludes this paper along with an outlook on future work.

2 The Longitudinal Finger Rotation Problem

Usually, finger-vein scanners are designed to capture only one finger at a time. For these scanners, finger misplacements are a severe problem. There are different types of misplacement: shifts of the finger in x- and y-direction (planar shifts), shifts of the finger in z-direction, in-plane (planar) rotation of the finger, tilts of the finger and rotation around the finger's longitudinal axis. The planar shifts as well as the planar rotations can be reduced by guiding walls alongside the finger, end tips or a finger-shaped support. Shifts of the finger in z-direction are usually not a problem if the sensor has a surface where the finger has to be placed onto. Remaining planar shifts and rotations can be compensated in software by aligning the images based on the finger outline. Tilts of the finger can be avoided by using capacitive or pressure-sensitive sensors on the scanner surface which detect if the finger is placed correctly. However, rotations around the finger's longitudinal axis cannot be detected reliably by most available commercial available sensors. This problem could be avoided if the sensors would not only acquire one finger, but require the subject to place the full hand or at least more than one finger, as proposed by Kauba et al. in [KPU18], on the sensor. Fig. 1 shows an example of the longitudinal finger rotation, also called non-planar rotation or out-plane rotation by some authors, using an off-the-shelf commercial finger vein scanner. In a supervised acquisition scenario, the supervisor can tell the user to place his finger correctly. However, if the acquisition is not supervised, such longitudinal rotations of the finger impose a severe problem. This problem gets worse if the scanner is designed to operate in a contact-less way and does not have a contact surface.

Fig. 1: Finger rotation example using a commercial scanner (rotation counter-clockwise)

The captured image is a projection of the finger situated in a 3D space onto a 2D plane. This principle is depicted in Fig. 2. If the finger is rotated around its longitudinal axis, the vein patterns look different due to the change in the perspective or the projection, respectively. This projective transformation cannot be reverted using translation or rotation on the images, but can be compensated to some degree if either the rotation angle is known or can be estimated. Estimating the rotation from a single image can be a challenging task. If the angle of rotation increases, some vein lines might merge due to the perspective projection. In this case, there is no way to revert the effects caused by the longitudinal finger rotation. Thus, it would be desirable if the recognition scheme is robust against longitudinal finger rotation, at least to a certain extent. To the best of our knowledge, until now the robustness against finger rotation has not been systematically evaluated.

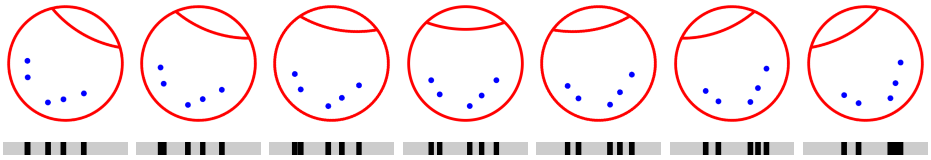

Fig. 2: Finger longitudinal axis rotation principle: a schematic finger cross section showing five veins (blue dots) rotated from $-30°$ (left) to $+30°$ (right) in $10°$ steps. The projection (bottom row) of the vein pattern is different according to the rotation angle following a non-linear transformation

3 PLUSVein-Finger Rotation Data Set

The finger rotation data set has been acquired using our custom designed multi-perspective finger vein scanner, shown in Fig. 3 right. The image sensor is an NIR enhanced industrial camera (IDS Imaging UI-1240ML-NIR), equipped with a 9 mm wide-angle-lens (Fujion HF9HA-1b) and a NIR long-pass filter (Midopt LP780). Five 808 nm NIR laser modules form the light source, positioned on the opposite side of the camera (transillumination), including an integrated automatic brightness control to achieve an optimal image contrast. To capture different perspectives or rotation angles, the camera and the illuminator rotate around the finger which is placed at the axis of rotation. This rotation principle is depicted in Fig. 3 left. The finger is stabilised with the help of a finger-tip shaped hole on the finger end and a height-adjustable finger trunk plate on the finger trunk. All parts except the camera, lens, filter and the laser modules were designed and manufactured by ourselves.

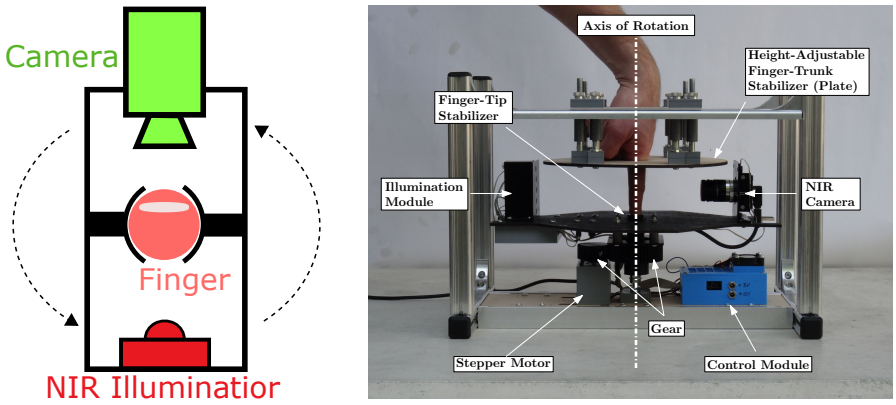

Fig. 3: Left: Principle of the multi-perspective finger vein scanner, right: the scanner itself (originally published in [PKU18], © 2018 IEEE)

The data set itself contains a total of 252 unique fingers from 63 different subjects, four fingers (right and left index and middle finger, respectively) per subject. Video sequences with a rotation speed adjusted to the frame rate were captured such that frames in $1°$ steps can be extracted in a range of $\pm 90°$ starting from the palmar view, by rotating the scanner around the finger's longitudinal axis. This leads to the same output images as if the finger would rotate itself. The capture process was repeated 5 times per finger. For each degree

of rotation there are 1260 images, resulting in 228060 images in total. Fig. 4 shows some example images in 10° steps and the corresponding extracted finger veins using Maximum Curvature [MNM07]. It becomes clearly visible that the extracted vein patterns are distinct among the different views (note the highlighted areas in the bottom row of the figure). The gender distribution of the volunteers is balanced. Among the 63 subjects 36 of the subjects are male, the remaining 27 are female. The youngest subject was 18, the oldest one 79. The image resolution is 650×1280 pixels.

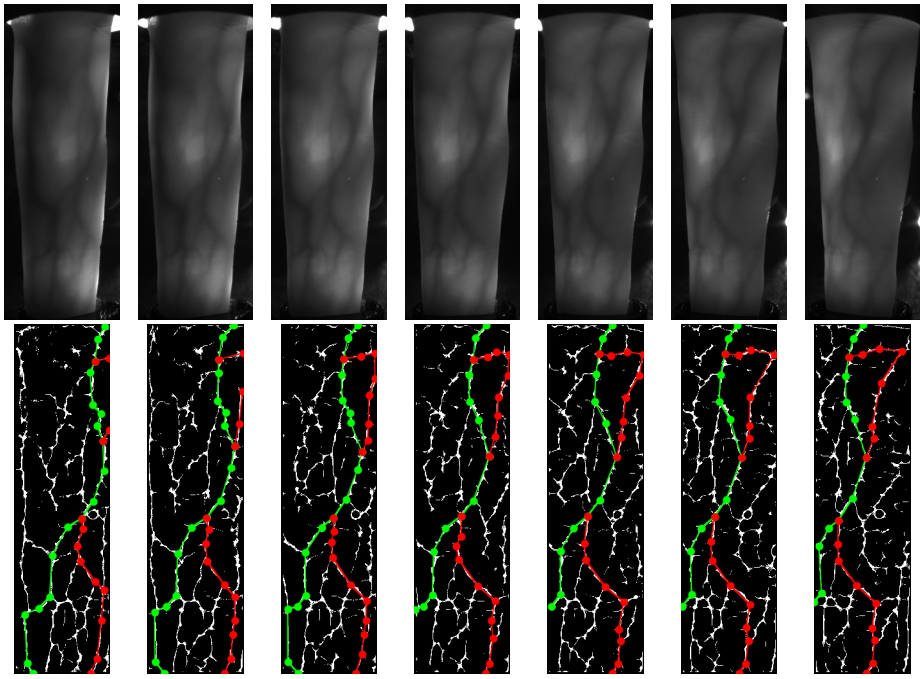

Fig. 4: Top: example images in 10° steps, from left to right: -30°, -20°, -10°, 0°, 10°, 20°, 30°, bottom: corresponding extracted MC features with two highlighted vein paths.

4 Experiments

Recognition Tool-chain: Fig. 5 shows the components of a biometric recognition system: The biometric trait is captured by a biometric sensor and afterwards processed in the recognition tool-chain which consists of preprocessing (ROI (region of interest) extraction and image enhancement), feature extraction and comparison. The input of our tool-chain are the videos captured by our mulit-perspecitve finger vein scanner. At first the frames corresponding to 1° steps are extracted from the video sequences. Afterwards each image is processed individually: the ROI is extracted and the the finger outline detected by the help of an edge detection algorithms. Then a straight centre line is fitted into the finger. Based on this centre line, the finger is aligned (rotated and shifted) such that it is in horizontal position in the middle of the image. The area outside the finger is masked out

(pixels set to black) and a rectangular ROI is fit inside the finger area. The ROI images have a size of 300×1100 pixels. To improve the visibility of the vein pattern we use **High Frequency Emphasis Filtering** (HFE), **Circular Gabor Filter** (CGF) and simple **CLAHE** (local histogram equalisation) as preprocessing. We opted for three well-established binarisation type feature extraction methods as well as two key-point based method. **Maximum Curvature** (MC) [MNM07], **Principal Curvature** (PC) [Ch09] and **Gabor Filter** (GF) [KZ12] aim to extract the vein pattern from the background resulting in a binary image, followed by a comparison of these binary images. Comparing the binary feature images is done using a correlation measure, calculated between the input images and in x- and y-direction shifted and rotated versions of the reference image. In addition, two key-point based recognition schemes, a **SIFT** [KRU14] based technique with additional key-point filtering and **Deformation-Tolerant Feature-Point Matching** (DTFPM) proposed by Matsuda et al. [Ma16] are used. For more details on the preprocessing methods please refer to [KRU14].

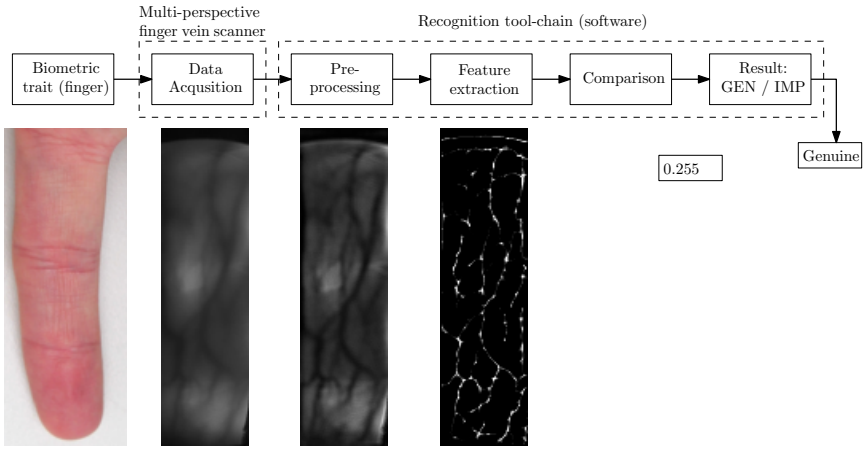

Fig. 5: Basic components of a biometric recognition system

Evaluation Protocol: To quantify the performance, the EER as well as the FMR1000 (the lowest FNMR for FMR $\leq 0.1\%$) and the ZeroFMR (the lowest FNMR for FMR $= 0\%$) are used. For calculating the genuine scores, all possible genuine comparisons are performed, which are $63 \cdot 4 \cdot 5 \cdot 5 = 6300$ comparisons. For calculating the impostor scores, only the first image of a finger is compared against the first image of all other fingers, resulting in $4 \cdot 63 \cdot 63 = 15876$ compares, so 22176 compares in total. An implementation of the complete processing tool-chain as well as the scores and detailed results are available at: `http://www.wavelab.at/sources/Prommegger18b/`.

Experimental Results: Table 1 lists the baseline performance results for the different finger-vein recognition schemes at the palmar view (0°). PC achieves the best recogniti-

on performance with an EER of 0.48%, followed by MC, DTFPM and SIFT while GF performs worst.

	PC	MC	DTFPM	SIFT	GF
EER [%]	0.48	0.59	1.15	1.53	3.14
FMR1000 [%]	0.79	0.83	2.54	4.88	5.40
ZeroFMR[%]	1.51	1.31	3.93	6.43	7.82

Tab. 1: Baseline performance results (palmar view, 0°) for the different recognition schemes

In order to quantify the robustness against longitudinal finger rotations, the images captured in the different angles from $-90°$ to $90°$ in $1°$ steps are compared against the palmar view (rotation of 0°). The trend of the absolute EER is shown in Fig. 6 left column. The relative performance degradation (RPD) $\left(\frac{EER_{rotated}-EER_{palmar}}{EER_{palmar}}\right)$ is depicted in the right column. The bottom row shows the area of $\pm 25°$ from the palmar view in more detail. Note that the RPD is calculated with respect to its baseline EER of each recognition scheme. As a result of this, the maximum RPD is limited by $RPD_{max} = \frac{EER_{max}-EER_{baseleine}}{EER_{baseline}}$ where EER_{max} is $\sim 50\%$.

MC (red line with triangular marker) and PC (green line with square marker) show a similar performance: up to a rotation angle of $\pm 10°$ the EER rises just above 1% which corresponds to a relative performance decrease about 100%. With increasing rotation angle, the recognition performance diminishes at a higher rate. At $\pm 10°$ the EER reaches 2%, between $\pm 20°$ and $\pm 25°$ the EER jumps above 10%. Around $\pm 30°$ the EER exceeds 30%, at $\pm 45°$ already 45%, i.e. recognition is no longer meaningful. DTFPM (brown line with star marker) has a higher baseline EER (1.15%) at the palmar view but its EER increases most gently, leading to the best robustness against finger rotation. At $\pm 10°$ the performance degradation is only 30% (EER: 1.53%). Starting from $\pm 17°$ DTFPM outperforms all other schemes. At $\pm 30°$ its EER is still below 7%. Matsuda et al. [Ma16] reported a baseline EER of 0.152% and a relative performance degradation of 230% (EER: 0.501%) at $\pm 30°$. However, neither their data set nor an implementation of their proposed approach is available. With our full re-implementation we are able to confirm their claimed robustness against finger rotation, but with a relative performance degradation of 500% instead of 230%. SIFT (blue line with diamond marker) is more robust against finger rotation than PC and MC, too. However, its baseline EER is higher than the one of DTFPM. GF (black line with cross marker) has the highest baseline EER (3.18%) and a similar relative performance degradation as MC and PC. Due to its high baseline EER, its RPD_{max} is lower than RPD_{max} for PC and MC. FMR1000 and ZeroFMR, visualized in Fig. 7, follow the same trend as the EER: first, the increase is relatively small and starts to rise sharply at $\pm 15°$. FMR1000 exhibits values close to 100 from $\pm 45°$ onwards for all algorithms evaluated, ZeroFMR already at $\pm 35°$. DTFPM shows the best results for both, FMR1000 and ZeroFMR. Consequently, a longitudinal finger rotation angle of $\pm 30°$ poses a severe problem for all evaluated schemes except DTFPM. A rotation angle of more than $\pm 45°$makes recognition nearly impossible.

To assist the reader in comparing the performance values at different rotation angles, Tab. 2 lists the EER per rotation angle from 0° - $\pm 45°$. The best EER for every rotation angle is

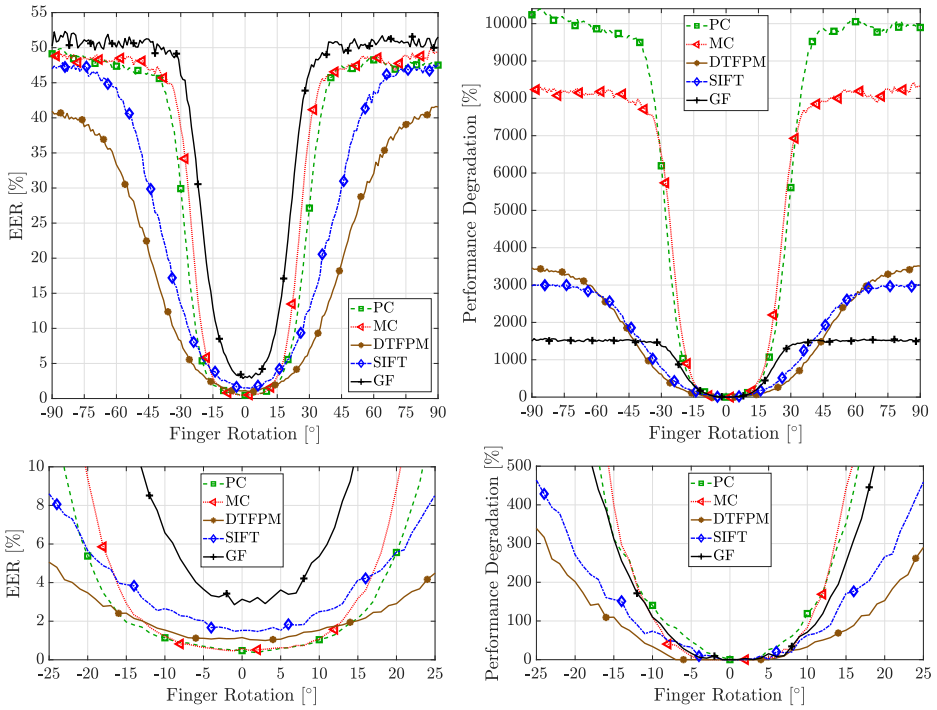

Fig. 6: Trend of performance indicators across the different rotation angles from −90° to 90° (0° corresponds to the palmar view), left: absolute EER values, right: relative change of EER in %. The bottom row shows a more detailed view from −25° to 25°.

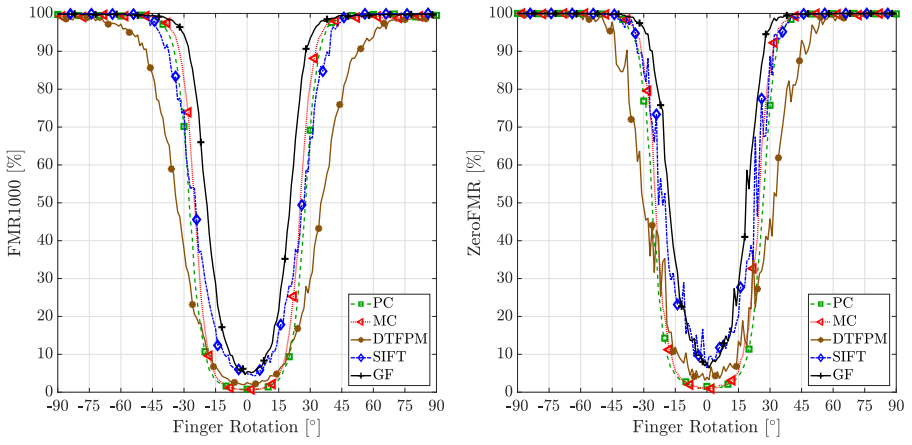

Fig. 7: Trend of performance indicators across the different rotation angles from −90° to 90° (0° corresponds to the palmar view), left: FMR1000, right ZeroFMR in %

highlighted **bold**. This table confirms that up to a certain rotation, the well established vein pattern based algorithms show the best performance. It can be seen that if the rotation exceeds a certain angle, key-point based algorithms, especially DTFPM, outperform traditional approaches.

	±0°	±5°	±10°	±15°	±20°	±25°	±30°	±45°
PC	**0.48**	**0.60**	**1.04**	**1.96**	5.38	13.43	27.14	46.50
MC	0.59	0.62	1.07	2.92	8.88	22.34	37.91	46.82
DTFPM	1.15	1.07	1.53	2.03	**2.91**	**4.49**	**6.97**	**19.26**
SIFT	1.53	1.53	2.49	3.90	5.59	8.53	12.61	30.15
GF	3.14	3.62	5.36	11.03	22.70	37.86	46.06	50.46

Tab. 2: EER at specific rotation angles [%]

Tab. 3 lists the relative performance degradation for the same rotation angles. With respect to RPD, DTFPM performs best followed by SIFT. Although GF shows the lowest RPD for ±45°, it has the worst recognition rate of all feature types, with an EER of $\sim 50\%$. The low RPD is due to the highest baseline result compared to the other feature types. The two tables (Tab. 2 and Tab. 3) clearly show that the evaluated key-point based algorithms are more tolerant against finger rotation than the vein pattern based ones. The key-point based algorithms match relevant key-points against each other instead of comparing binarised vein structures. If the detection and matching of theses points is insensitive to changes in the vein patterns due to longitudinal finger rotation, the results of a comparison in a biometric recognition system is less sensitive as well.

	±0°	±5°	±10°	±15°	±20°	±25°	±30°	±45°
PC	**0**%	26%	119%	312%	1031%	2727%	5610%	9684%
MC	**0**%	7%	83%	399%	1416%	3715%	6373%	7894%
DTFPM	**0**%	**0**%	**33**%	**76**%	**153**%	**290**%	**505**%	1573%
SIFT	**0**%	**0**%	63%	155%	266%	459%	726%	1876%
GF	**0**%	15%	71%	252%	624%	1107%	1369%	**1509**%

Tab. 3: Relative performance degradation at specific rotation angles [%]

Tab. 4 is the inverse of Tab. 3 and shows rotation angle at which a certain performance drop is hit. While vein pattern based algorithms (MC, PC, GF) reach 100 performance decrease around ±10°, key-point based systems tolerate higher rotation angles, e.g. DTFPM reaches a RPD of 100% at 14°. The further the finger is rotated, the more pronounced this trend becomes: the relative performance decrease of SIFT and especially DTFPM is lower than the one of PC, MC and GF. DTFPM exceeds a RPD of 500% at 28° whereas for PC, MC and GF this performance decrease is already achieved just above ±15°.

5 Conclusion

We investigated the problem of finger rotation around its longitudinal axis, also called non-planar or out-plane rotation of the finger in the scope of finger-vein recognition. This kind of finger misplacement poses a severe problem for practical applications of finger-

	10%	25%	50%	100%	200%	300%	400%	500%
PC	±1°	±3°	±5°	±8°	±12°	±13°	±15°	±16°
MC	±5°	±6°	±8°	±9°	±12°	±13°	±14°	±15°
DTFPM	±**7**°	±**8**°	±**11**°	±**14**°	±**19**°	±**23**°	±**26**°	±**28**°
SIFT	±4°	±4°	±8°	±12°	±16°	±20°	±23°	±25°
GF	±4°	±5°	±7°	±9°	±12°	±14°	±16°	±17°

Tab. 4: Rotation angle at which a certain relative performance degradation is hit

vein scanners, including most of the available off-the-shelf single finger commercial finger vein scanners, as this rotation cannot be prevented by means of the scanner hardware construction and is hard to be compensated afterwards by image preprocessing (assuming that the rotation angle is not known). We established a new finger rotation data set comprising finger-vein images captured in 1° steps of longitudinal rotation in a range of ±90° starting from the palmar view.

Our performance evaluation results confirm, that longitudinal finger rotation is a severe problem for the recognition performance of finger-vein systems. All recognition schemes are able to tolerate up to ±10° of rotation at a relative performance loss of less than 120%. The key-point based algorithms DTFPM and SIFT are more robust against finger rotation, but their baseline performance is worse compared to PC and MC. GF generally performs worst. However, for rotation angles more than 30°, which can occur in practical applications of finger-vein scanners, the recognition performance drops dramatically. This problem gets even worse for touchless finger-vein scanners with more degrees of freedom during image acquisition.

If only the planar finger-vein images are available, the ability of a recognition scheme to cope with longitudinal rotation of the finger is very limited due to the perspective mapping during imaging. One way to make finger-vein recognition more robust against finger rotation is by improving the scanner hardware, e.g by mounting an additional finger positioning support where the whole hand is placed on a kind of shelf such that the rotation of the finger can be restricted. Another option is using stereo or 3D camera systems, which is beneficial for touchless scanners anyway, in order to estimate the rotation angle of the finger and compensate for the rotation by applying a perspective transform. Another way is trying to estimate the rotation angle and compensate the rotation like Chen et al. [Ch18] proposed, which will be evaluated in our future work.

For our data set the exact longitudinal finger rotation is known. This information can be used to perform a systematic evaluation of the approach in [Ch18]. A further approach is to correct the perspective distortion by applying a non-linear transform using the known rotation angle. We will evaluate the recognition performance which can be retained at certain rotation angles for both approaches in order to determine the maximum possible rotation angle at which a reasonable recognition is still feasible.

Acknowledgements

This project has received funding from the European Union's Horizon 2020 research and innovation program under grant agreement No. 700259.

References

[Ch09] Choi, Joon Hwan; Song, Wonseok; Kim, Taejeong; Lee, Seung-Rae; Kim, Hee Chan: Finger vein extraction using gradient normalization and principal curvature. volume 7251, pp. 7251 – 7251 – 9, 2009.

[Ch18] Chen, Qing; Yang, Lu; Yang, Gongping; Yin, Yilong: Geometric shape analysis based finger vein deformation detection and correction. Neurocomputing, 2018.

[KPU18] Kauba, Christof; Prommegger, Bernhard; Uhl, Andreas: The Two Sides of the Finger - Dorsal or Palmar - Which One is Better in Finger-Vein Recognition? In: Proceedings of the International Conference of the Biometrics Special Interest Group (BIOSIG'18). Darmstadt, Germany, 2018.

[KRU14] Kauba, Christof; Reissig, Jakob; Uhl, Andreas: Pre-processing cascades and fusion in finger vein recognition. In: Proceedings of the International Conference of the Biometrics Special Interest Group (BIOSIG'14). Darmstadt, Germany, sep 2014.

[KZ12] Kumar, Ajay; Zhou, Yingbo: Human identification using finger images. Image Processing, IEEE Transactions on, 21(4):2228–2244, 2012.

[Ma16] Matsuda, Yusuke; Miura, Naoto; Nagasaka, Akio; Kiyomizu, Harumi; Miyatake, Takafumi: Finger-vein authentication based on deformation-tolerant feature-point matching. Machine Vision and Applications, 27(2):237–250, 2016.

[MNM07] Miura, Naoto; Nagasaka, Akio; Miyatake, Takafumi: Extraction of finger-vein patterns using maximum curvature points in image profiles. IEICE transactions on information and systems, 90(8):1185–1194, 2007.

[PKU18] Prommegger, Bernhard; Kauba, Christof; Uhl, Andreas: Multi-Perspective Finger-Vein Biometrics. In: Proceedings of the IEEE 9th International Conference on Biometrics: Theory, Applications, and Systems (BTAS2018). Los Angeles, California, USA, pp. 1–9, 2018.